Analyst

ROYAL SOCIETY OF CHEMISTRY

MINIREVIEW

View Article Online
View Journal | View Issue

Cite this: *Analyst*, 2022, **147**, 1257

Semiconductor-based surface enhanced Raman scattering (SERS): from active materials to performance improvement

Xuejiao Wang, [a] Erjin Zhang,*[b] Huimin Shi, [c] Yufeng Tao[a] and Xudong Ren*[a]

Surface enhanced Raman scattering (SERS) is a powerful spectral analysis technique and has exhibited remarkable application prospects in various fields. The design and fabrication of high-performance SERS substrates is key to promoting the development of SERS technology. Apart from noble metal substrates, non-metal substrates based on semiconductor materials have received increasing attention in recent years owing to their unique physical, chemical, and optical properties. However, compared with noble metal substrates, most semiconductor substrates show weak Raman enhancement ability. Therefore, exploring effective strategies to improve the SERS sensitivity is an urgent task. Numerous reviews have outlined the research progress of semiconductor SERS substrates, which mainly focused on summarizing the material category of semiconductor substrates. However, reviews that systematically summarize the strategies for improving the SERS performance of semiconductor substrates are lacking. In this review, we comprehensively discuss the research on semiconductor SERS from the aspects of mechanism, materials, and modification. Firstly, the Raman enhancement mechanism of semiconductor substrates and the SERS-active materials are discussed. Then, we summarize several effective approaches to boost the SERS performance of semiconductor substrates. In conclusion, we propose some prospects for this field.

Received 30th November 2021,
Accepted 22nd February 2022

DOI: 10.1039/d1an02165f

rsc.li/analyst

1 Introduction

Surface-enhanced Raman scattering (SERS) was first discovered by Fleischmann *et al.* in 1974 on the rough surface of a silver electrode.[1] As a powerful spectroscopic technique, SERS achieves ultratrace detection by amplifying the Raman signal of molecules and possesses the advantages of high sensitivity, fingerprint specificity, and non-destructive detection. SERS

[a]*Institute of Micro-Nano Optoelectronics and Terahertz Technology, School of Mechanical Engineering, Jiangsu University, Zhenjiang 212013, People's Republic of China. E-mail: zhej@ujs.edu.cn, renxd@ujs.edu.cn*
[b]*Institute for Energy Research, Jiangsu University, Zhenjiang 212013, People's Republic of China*
[c]*College of Physics and Electronic Engineering, Northwest Normal University, Lanzhou 730070, People's Republic of China*

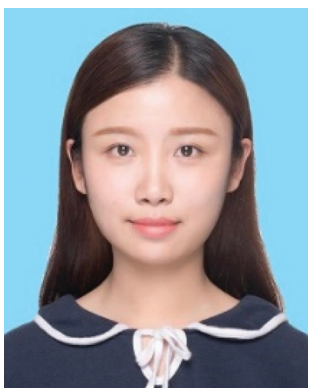

Xuejiao Wang

Xuejiao Wang received her Ph.D. from the College of Computer Science and Electronic Engineering, Hunan University in 2020. She joined Jiangsu University, China, in 2020. Currently, she is an assistant professor at the Institute of Micro-Nano Optoelectronics and Terahertz Technology, Jiangsu University, China. Her research interests focus on the fabrication and application of highly sensitive surface-enhanced Raman spectroscopy (SERS) substrates.

Erjin Zhang

Erjin Zhang received his Ph.D. from the School of Physics and Electronics, Hunan University in 2020. He joined Jiangsu University, China, in 2020. Currently, he is an assistant professor at the Institute for Energy Research, Jiangsu University, China. His current research direction is the design, synthesis, and application of functional materials in energy storage and conversion, and in situ *Raman analysis of electrochemical reaction mechanisms.*

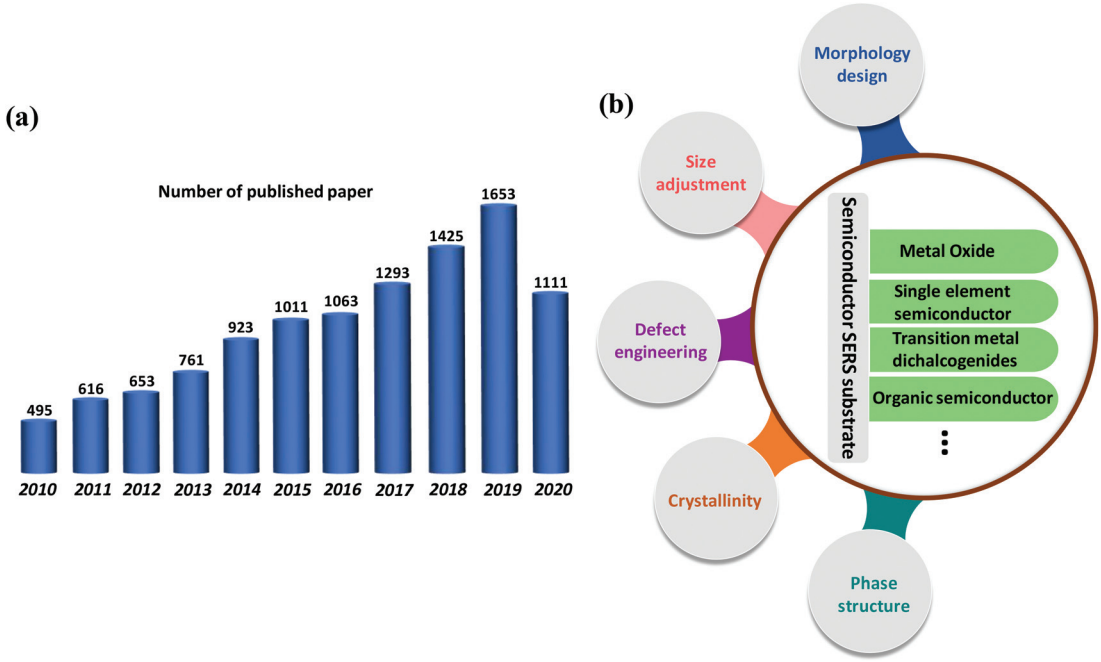

Fig. 1 (a) Published papers related to semiconductor SERS in recent years (the data comes from *Web of Science* by searching the key word "semiconductor enhance Raman"). (b) Overview of this review.

has been widely used in various fields such as chemical and biological analysis,[2,3] medical diagnosis,[4,5] environmental analysis,[6,7] food safety,[8,9] and artwork restoration.[10] At present, the widely accepted SERS enhancement mechanism includes the electromagnetic enhancement mechanism (EM) and the chemical enhancement mechanism (CM). The EM means that the strong electromagnetic field generated by the localized surface plasmon resonance (LSPR) of metal nanostructures can realize the Raman signal enhancement. The CM is relatively complex, mainly based on the charge transfer between the SERS substrate and the molecule adsorbed on its surface to achieve the Raman signal enhancement.[11]

The SERS substrate is the core of SERS technology, and has extended from noble metals (Au, Ag, and Cu) and transition metals to semiconductor materials.[12,13] In fact, the noble metal SERS substrate has always been dominant because it possesses an extremely high SERS enhancement factor (EF) (10^{10}–10^{12}) to achieve ultrasensitive and even single-molecule-level detection. However, there are some inevitable disadvantages for noble metal SERS substrates, such as poor stability, easy oxidation, high cost, poor reproducibility and biocompatibility, and lack of selective recognition ability for probe molecules.[14] In addition, the strong photothermal effect at "hot spots" may cause significant damage to living cells.[15] Semiconductor SERS substrates have been extensively studied in recent years.[16] Fig. 1a indicates that the publications related to semiconductor SERS have increased in recent years. Compared to noble metal SERS substrates, semiconductor

Huimin Shi

Huimin Shi received his Ph.D. in Physics from Hunan University in 2018. Currently, he is an assistant professor at the School of Mechanical and Electrical Engineering, Guangzhou University, China. His research interests include the synthesis of nanomaterials, micro/nanomanufacturing and their relevant applications.

Yufeng Tao

Yufeng Tao received his Ph.D. from Nanjing Normal University in 2017. He completed his postdoctoral work at Huazhong University of Science and Technology in 2020. Currently, he is an assistant professor at the Institute of Micro-Nano Optoelectronics and Terahertz Technology, Jiangsu University, China. His research is focused on micro/nano optoelectronic devices and nanosensors.

substrates show better chemical stability, rich variety, and low price.[16,17] Some semiconductor materials have excellent photocatalytic degradation ability, so the SERS substrate can be reused to improve the reproducibility of the SERS signal.[18,19] Moreover, semiconductor substrates have better biocompatibility, exhibiting great application potential in life sciences. The selective Raman enhancement property enables semiconductor SERS substrates to recognize and detect target molecules in a complex environment.[20] Significantly, the physical and chemical properties of semiconductor substrates such as exciton Bohr radius, band structure, and carrier concentration are easy to regulate.[21] The above advantages can compensate for the bottleneck of noble metal SERS substrates. However, the EF of semiconductor substrates is generally low ($10–10^2$), hindering their practical applications.[22] Therefore, developing novel SERS-active semiconductor materials and further improving the SERS performance of semiconductor substrates by adjusting their morphology, size, surface state, crystalline state, *etc*. is significant.

In this review, we focus on providing an overview of the strategies for enhancing the SERS performance of semiconductor substrates. We start with a brief introduction to several main types of semiconductor SERS substrates, including metal oxides, single element semiconductors, transition metal dichalcogenides, and organic semiconductors. As a guideline for semiconductor substrate design, the enhancement mechanism of semiconductor SERS substrates is also discussed. Next, as the core part of this review, we discuss various effective strategies for enhancing the SERS performance of semiconductor substrates such as adjusting the morphology, size, defect state, crystallinity, and phase structure. We mainly focus on the fabrication methods of these substrates and the working principle behind the enhanced SERS performance. Finally, we summarize the current development and challenges of semiconductor SERS substrates, and further highlight the prospects of semiconductor substrates from the aspect of design, fabrication and mechanism. Fig. 1b shows the overview of this mini-review.

Xudong Ren

Xudong Ren received his Ph.D. from Jiangsu University in 2009. He is currently a full professor at the School of Mechanical Engineering, Jiangsu University, China. His current research is concerned with laser advanced manufacturing and micro/nano optoelectronic devices.

2 A brief introduction to semiconductor SERS substrates

2.1 Enhancement mechanism of semiconductor SERS substrates

The free electrons in noble metals are prone to generate the LSPR effect under incident light excitation, so the enhancement mechanism of noble metal SERS substrates mainly originates from electromagnetic enhancement. In contrast, semiconductor substrates show a relatively complex mechanism. According to existing research results, the enhancement mechanism of semiconductor SERS substrates includes both EM and CM[13] (Fig. 2).

2.1.1 Electromagnetic enhancement. We know that electromagnetic enhancement is generated by LSPR. The surface plasmon resonance frequency of semiconductor materials is proportional to the electron density.[21] Therefore, the LSPR peak of semiconductors is located in the infrared and ultraviolet region due to the generally low electron density of the conduction band (CB) and large electron density ($10^{22}–10^{24}$ cm^{-3}) of the valence band (VB), indicating that LSPR hardly contributes to the SERS of semiconductors in the visible light region.[23] Fortunately, optimizing the geometry configuration and size, and modulating the carrier concentration *via* defect engineering are facile strategies to manipulate the surface plasmon resonance frequency of semiconductor substrates, resulting in the generation of LSPR effect in the visible light region.[24,25] Fig. 2a presents the LSPR generation in semiconductor materials by controlling doping. Maznichenko *et al.* found that the plasmon resonance of rutile TiO_2 shifted from vacuum–ultraviolet region to 532 nm by fabricating a 3D TiO_2 nanofiber network.[26] In addition, Mie-resonance is an optical resonance of whispering gallery modes (WGMs). For semiconductor substrates with a large and uniform size, optical microcavity structure of ring or ring-like cavity and high refractive index, the Mie-resonance provides local electromagnetic field enhancement to boost the Raman signal of adsorbed molecules.[27] Hayashi *et al.* first applied Mie scattering effect to semiconductors in 1988.[28]

2.1.2 Chemical enhancement. Compared to electromagnetic enhancement mechanism, chemical enhancement plays a more crucial role in the Raman enhancement of semiconductor substrates. Chemical enhancement mainly involves charge transfer and exciton resonance enhancement (Fig. 2b). The charge transfer process may occur from the semiconductor to the adsorbed molecules, or from the adsorbed molecules to the semiconductor. When the highest occupied molecular orbital (HOMO) and lowest unoccupied molecular orbital (LUMO) of the molecule match the VB and CB energy levels of the substrate, effective charge transfer process will occur between them, and the molecular polarizability and electron density distribution will change, resulting in the SERS effect.[11,29] But this is usually not the case, so the semiconductor materials often exhibit poor SERS performance. Fortunately, various strategies have been developed to regulate

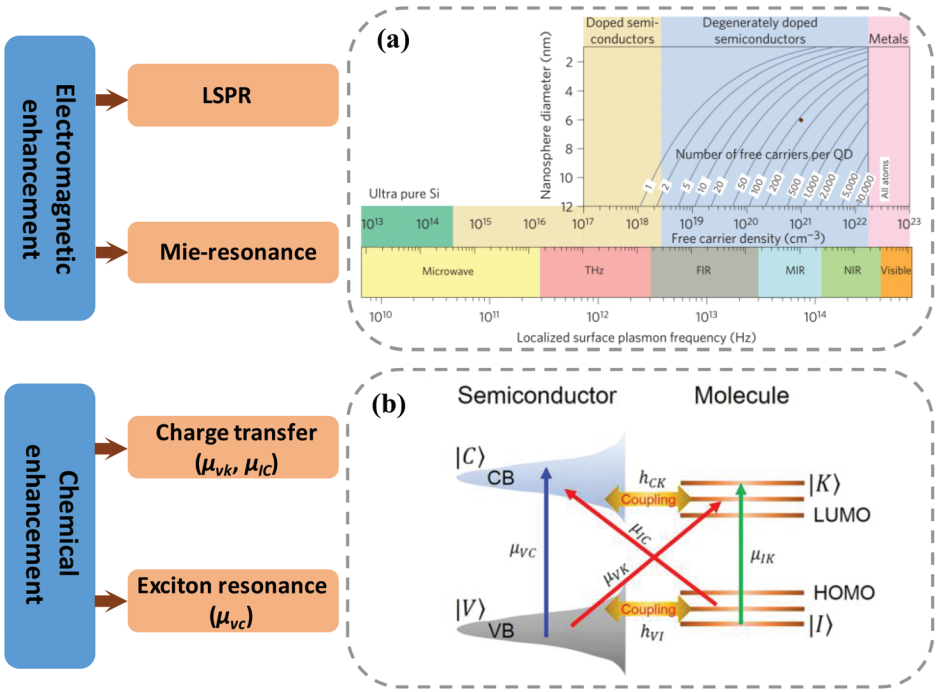

Fig. 2 Raman enhancement mechanism of semiconductor substrates. (a) The regulation of localized surface plasmon frequency by doping. Reproduced with permission from ref. 24 (Copyright © 2011, Nature Publishing Group). (b) The charge transfer process in a semiconductor–molecule system. Reproduced with permission from ref. 29 (Copyright © 2019, American Chemical Society).

the energy level distribution of semiconductor substrates to enhance the charge transfer process. Charge transfer in a semiconductor–molecule system generally involves the following pathways[11,30–32]: (1) Molecule HOMO-to-CB; (2) Charge transfer complex-to-CB; (3) VB-to-molecule LUMO; (4) VB-to-surface state-to-molecule LUMO; and (5) CB-to-molecule HOMO. Since some articles have discussed the above charge transfer process in depth,[11,12,33] this review will not discuss it in detail. Apart from the charge transfer, exciton resonance may also affect the SERS performance of semiconductor materials. Specifically, under optical excitation, electrons transition from the VB to CB and generate electron–hole pairs named excitons. The distance of the electron–hole pair represents the exciton Bohr radius. When the size of the semiconductor nanoparticle is smaller than the exciton Bohr radius, the exciton levels tend to diverge so that only specific transition energies are allowed, and the "band gap" (lowest-energy optical transition) shifts to higher energies, resulting in the size dependence of spectra and a change of the charge transfer process in the semiconductor–molecule system.[34,35] In fact, the SERS performance of semiconductors may be improved when the frequency of the incident light is close to the exciton resonance frequency.

2.2 Enhancement factor calculation

The EF is an important parameter for SERS performance evaluation. The definition of the EF is highly diverse including the single molecule enhancement factor, the SERS-active substrate enhancement factor, and the analytical enhancement factor. The SERS-active substrate enhancement factor is the most commonly used method to evaluate SERS performance and is defined as follows:

$$\mathrm{EF} = \frac{I_{\mathrm{SERS}}/N_{\mathrm{SERS}}}{I_{\mathrm{Raman}}/N_{\mathrm{Raman}}}$$

where I_{SERS} is the SERS intensity, I_{Raman} is the classical Raman intensity obtained without the SERS substrate, and N_{SERS} and N_{Raman} stand for the number of molecules from the SERS substrate and classical Raman under laser illumination, respectively.

One of the difficulties in calculating the EF lies in the precise determination of N_{SERS} because it is a tricky business to accurately obtain the surface coverage of target molecules and the surface area of SERS substrate.[36] It should be noted that the accurate calculation of the EF requires that each parameter (I_{SERS}, I_{Raman}, N_{SERS}, N_{Raman}) be measured accurately. However, in actual calculation, some parameters are difficult to obtain accurately, and reasonable assumptions are required. There may be large differences in the EF obtained by different research groups. Therefore, more reliable methods need to be explored to evaluate SERS performance.

2.3 Semiconductor SERS substrates

Since the first observation of the SERS effect on the semiconductors NiO and TiO_2 surface in 1982 by Yamada *et al.*,[37,38] the species of semiconductor SERS substrates have become more abundant. More and more researchers are working on developing novel semiconductor SERS-active materials and

further improving their SERS performance. In this part, we summarize several well-developed types of semiconductor SERS substrates in recent years, including metal oxides, single element semiconductors, transition metal dichalcogenides, and organic semiconductors.

2.3.1 Metal oxides. Semiconducting metal oxide materials have been extensively applied in the SERS field due to the advantages of low cost, easy preparation, and high stability. Research studies have shown that many metal oxide materials exhibit SERS activity including ZnO, TiO_2, Fe_2O_3, Cu_2O, MoO_2, WO_3, VO_2, Nb_2O_5, Ta_2O_5, *etc*.[39] ZnO is a high refractive index semiconductor material and shows obvious merits as a SERS substrate.[40–42] Wen *et al.* observed the SERS effect of pure ZnO colloids using a cyanine dye D266 as probe molecules in 1996.[43] Researchers have designed and fabricated ZnO nanostructure with various morphologies to realize enhanced SERS activity. Liu *et al.* successfully synthesized parallelogram-shaped porous ZnO nanosheets and obtained a low SERS detection limit for 4-Mercaptobenzoic acid (4-MBA) molecules.[44] Zhang *et al.* prepared ZnO submicron flowers and demonstrated that this substrate could be employed as a SERS biosensor to detect heavy metal ions[45] (Fig. 3a). Moreover, TiO_2 is also a widely used semiconductor SERS material. Utilizing the excellent catalytic property of TiO_2 to introduce it into the SERS substrate can realize the reuse of the substrate and solve the poor reproducibility issue to a certain extent. Yang *et al.* fabricated flexible hydrogenated TiO_2 nanowires and studied the effect of hydrogenation on SERS performance and recyclability[46] (Fig. 3b). Fig. 3c presents the Cu_2O concave sphere fabricated by a template method, which possesses a high EF (2.8×10^5) and low detection limit (2×10^{-8} mol L^{-1}).[47] The MoO_2 monocrystalline ultrathin porous nanosheets exhibited high SERS activity,[48] as shown in Fig. 3d. It is worth noting that Ta_2O_5 and Nb_2O_5 have great potential in SERS as novel semiconductor substrates[49,50] (Fig. 3e and f).

2.3.2 Single element semiconductors. It has been proved that some single element semiconductor materials also display SERS activity including graphene, Si, Ge, *etc*. Since the discovery of graphene, it has been widely used in many fields due to its excellent optical, electrical, and mechanical properties. Ling *et al.* first reported the SERS phenomenon on graphene surface in 2010[51] (Fig. 4a). They further investigated the relationship

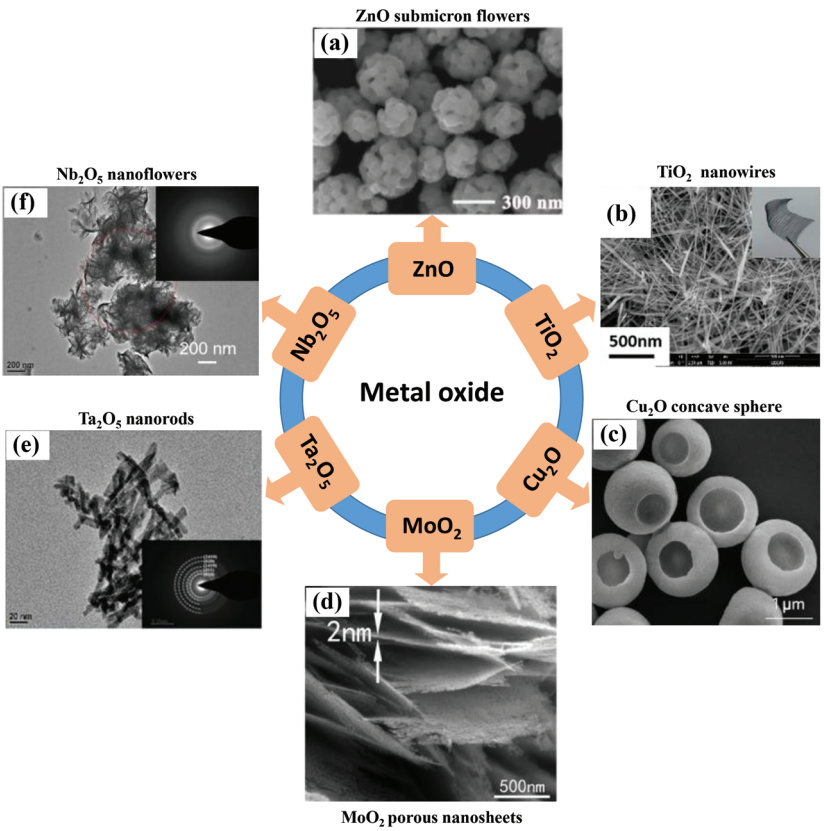

Fig. 3 (a) SEM image of ZnO submicron flowers. Reproduced with permission from ref. 45 (Copyright © 2021 Elsevier B.V. All rights reserved). (b) SEM image of TiO_2 nanowires. Reproduced with permission from ref. 46 (Copyright © 2018, American Chemical Society). (c) SEM image of Cu_2O concave sphere. Reproduced with permission from ref. 47 (Copyright © 2018 WILEY-VCH Verlag GmbH & Co. KGaA, Weinheim). (d) SEM image of MoO_2 monocrystalline ultrathin porous nanosheets. Reproduced with permission from ref. 48 (Copyright © 2019, Royal Society of Chemistry). (e) and (f) TEM image of Ta_2O_5 nanorods and Nb_2O_5 nanoflowers, insets are the corresponding selected area electron diffraction patterns. Reproduced with permission from ref. 49 and 50 (Copyright © 2019 The Authors. Published by WILEY-VCH Verlag GmbH & Co. KGaA, Weinheim; Copyright © 2020 The Authors. Published by Elsevier Ltd).

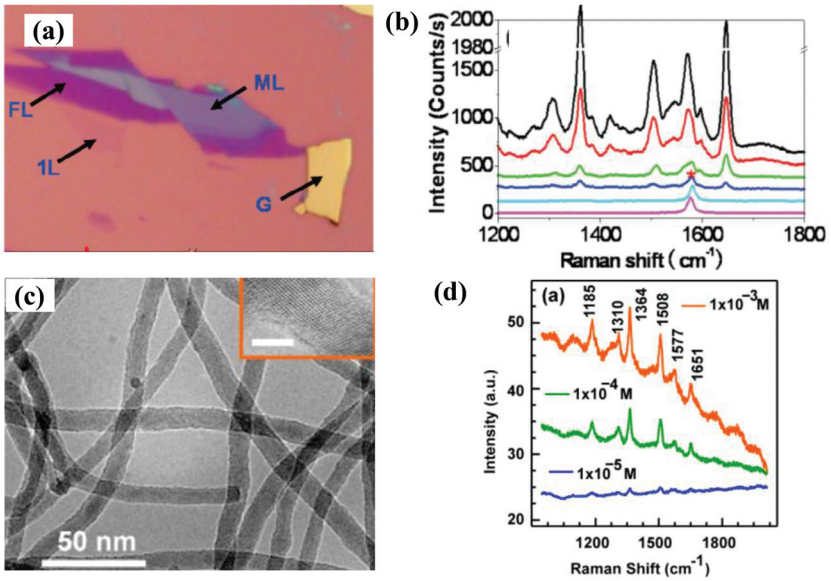

Fig. 4 (a) Optical image of graphene (single layer, few layers, and multilayer) and graphite. (b) SERS spectrum of Rhodamine 6G (R6G) molecules adsorbed on monolayer graphene (blue line), multilayer graphene (green line), and graphite (red line) substrates. Reproduced with permission from ref. 51 (Copyright © 2010, American Chemical Society). (c) TEM image of Si nanowires; the inset shows the HRTEM image of a typical Si nanowire. (d) SERS spectra of the R6G molecules adsorbed onto the Si nanowire substrate. Reproduced with permission from ref. 55 (Copyright © 2017, American Chemical Society).

between the molecular Raman signal and the number of graphene layers, suggesting that fewer layers lead to a stronger signal (Fig. 4b). On the basis of the above research, a variety of graphene-based SERS substrates such as graphene/metal composite structure and heterostructure have been developed.[52–54] In addition, Cui *et al.* fabricated the three-dimensional Si nanowire network structure, as shown in Fig. 4c. They demonstrated that the Si nanowire can act as a SERS platform[55] (Fig. 4d).

2.3.3 Transition metal dichalcogenides. Transition metal dichalcogenides is a kind of semiconductor material with MX_2 composition, where M represents a transition metal element and X is a chalcogen element. It has tunable thickness, interlayer gap, and phase structure, resulting in many excellent photoelectric properties including SERS.[56–59] Ultrathin 2D NbS_2 was synthesized by a chemical vapor deposition method and proved to be an excellent SERS substrate[60] (Fig. 5a and b). The authors revealed that the Raman enhancement originated from the high density of states near the Fermi level using density functional theory calculations. MoS_2 is one of the most concerned materials in the transition metal dichalcogenide family due to its easy preparation, high stability, and unique optical properties. Li *et al.* investigated the SERS performance of MoS_2 with different interlayer distances for the first time, finding that a smaller interlayer distance could realize better Raman enhancement[61] (Fig. 5c and d). Moreover, ReS_2, WTe_2, and WSe_2 can also be exploited as SERS-active materials[62–64] (Fig. 5e).

2.3.4 Organic semiconductors. Apart from inorganic semiconductor materials, researchers explored the possibility of organic semiconductors as a SERS platform.[13] The organic semiconductors have significant applications in the field of effect transistors and solar batteries due to their fascinating photoelectric properties. However, the SERS-related research is lacking. In fact, organic semiconductor films possess some attractive properties such as structural versatility, facile synthesis, and tunable optoelectronic properties, which is beneficial for designing target-specific SERS platforms. Demirel *et al.* innovatively employed a nanostructured organic semiconductor film (DFP-4T) as a SERS substrate[65] (Fig. 6a). This SERS platform presented a larger Raman enhancement factor and a low limit of detection, which is comparable to the intrinsic plasmonic metal-based SERS platforms. Fig. 6b shows the SERS spectra of MB on nanostructured DFP-4T film at different concentrations. Ganesh *et al.* demonstrated that quantum scale organic semiconductors can be used as a SERS probe to detect single-molecule DNA. In addition, this SERS probe can also trace the expression of two genes which are frequently used as cancer stem cells markers.[66] Fig. 6c and d presents the TEM image of a quantum organic semiconductor and the schematic of genomic DNA detection on the quantum organic semiconductor, respectively. These studies provide useful guidance for the design of organic semiconductor SERS substrate.

3 Approaches for enhancing the SERS performance of semiconductor substrates

Despite the semiconductor materials discussed in the previous section displaying SERS activity, the SERS performance is

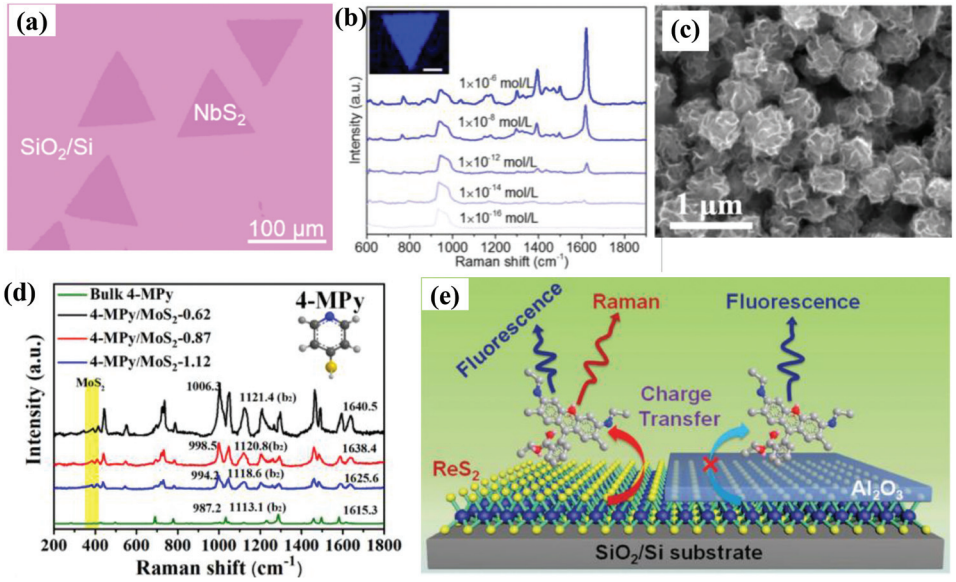

Fig. 5 (a) Optical image of 2D NbS_2 on SiO_2/Si substrate. (b) SERS spectra of different concentrations of methylene blue (MeB) molecules adsorbed on NbS_2 substrate; the inset is the SERS mapping of a single NbS_2 flake. Reproduced with permission from ref. 60 (Copyright © 2019, American Chemical Society). (c) SEM image of the MoS_2 nanoflowers. (d) SERS spectra of 4-mercaptopyridine (4-MPy) adsorbed on MoS_2 with different interlayer distances. Reproduced with permission from ref. 61 (Copyright © 2020, American Chemical Society). (e) Schematic showing the work principle of ReS_2 nanosheets as SERS platform. Reproduced with permission from ref. 64 (Copyright © 2018 WILEY-VCH Verlag GmbH & Co. KGaA, Weinheim).

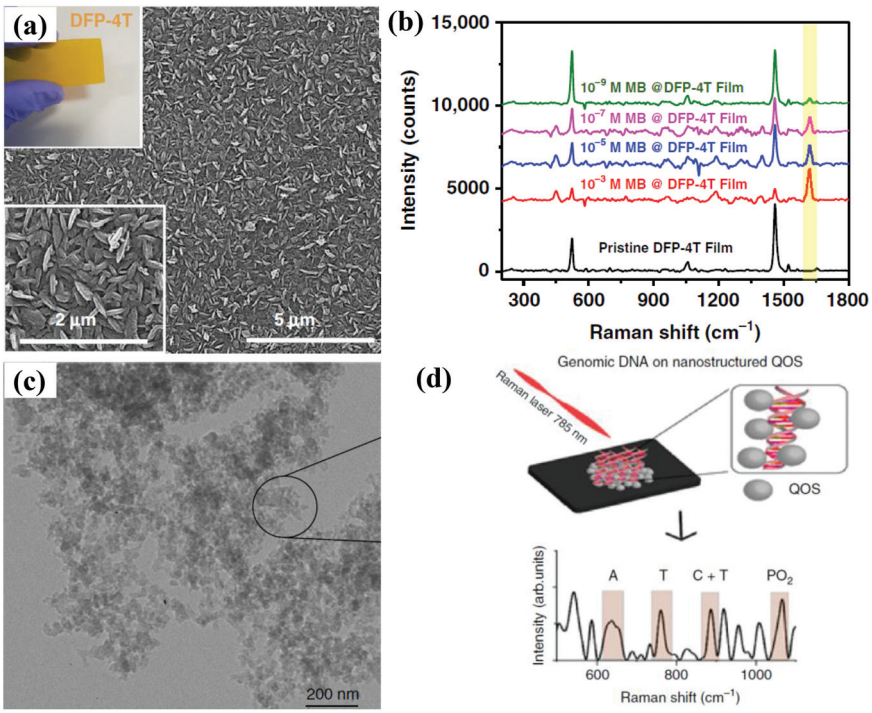

Fig. 6 (a) SEM image of the DFP-4T film; the top inset shows the optical image of the DFP-4T film. (b) SERS spectra of MB molecules adsorbed on nanostructured DFP-4T film at different concentrations. Reproduced with permission from ref. 65 (Copyright © 2019, the author(s)). (c) TEM image of a quantum organic semiconductor. (d) The schematic of genomic DNA detection on a quantum organic semiconductor. Reproduced with permission from ref. 66 (Copyright © 2020, the author(s)).

usually poor for most pure semiconductor materials.[67–70] Therefore, how to obtain highly sensitive semiconductor substrates is the essential issue to promote its practical applications. In this section, we discuss several strategies to enhance the SERS performance of semiconductor substrates mainly in the aspect of regulation mechanism. Table 1 shows

Table 1 SERS performance of some typical semiconductor substrates

	SERS substrate	Improvement strategy	Probes	EF	Ref.
Pure semiconductor materials	TiO_2 nanoparticles	—	4-MBA	$1–10^2$	67
	ZnO nanocrystal	—	4-MPy	10^3	68
	CuO nanocrystal	—	4-MPy	10^2	69
	Graphene	—	Dye molecules	2–17	51
	CdS nanoparticles	—	4-MPy	10^2	70
Performance improvement	Hollow multi-shelled V_2O_5 microstructure	Morphology design	MB	1.18×10^6	86
	Sea urchins-like MoO_3	Morphology design	R6G	10^5	87
	Graphene quantum dots	Size adjustment	Dye molecules	2730	92
	ZnO superstructure	Size adjustment	4-MPy	10^5	96
	Ga-doped ZnO nanoparticles	Defect engineering	MPy	6.66×10^4	107
	$W_{18}O_{49}$ nanowires	Defect engineering	R6G	3.4×10^5	107
	Amorphous TiO_2 Nanosheets	Crystallinity	4-MBA	1.86×10^6	29

the SERS performance of pure semiconductor nanocrystals and semiconductor substrates using improvement strategies, from which we can see that these strategies can effectively enhance the SERS performance of semiconductor substrates.

3.1 Morphology design

The Raman enhancement of noble metals strongly depends on LSPR, so structural design is an effective method to regulate their plasma properties and construct "hot spots". For example, the tip metal nanostructures with a small radius of curvature are prone to generating strong local electromagnetic fields due to the "lightning rod" effect.[71] Some metal nanostructures with rough surface or tiny nanogaps also contain abundant "hot spots".[72–74] Similar to noble metal nanostructures, the plasmon resonance of semiconductors can be manipulated by morphology design and optimization to enhance the SERS performance.[75] Benefiting from the abundant species and mature synthesis technology, various semiconductor nanostructures ranging from 0D (quantum dot, nanocrystalline),[68,76] 1D (nanowire, nanorod, nanocone),[77,78] and 2D (nanoplate, nanodisk)[79,80] to 3D (nanocage, nanoflower, nanoarray)[81,82] have been developed. Fu *et al.* synthesized α-Fe_3O_4 nanocrystals with different morphologies and explored the influence of morphology on SERS performance. They found the enhancement ability was nanospheres > nanospindles > nanocubes, indicating the great influence of morphology on SERS activity.[83] Semiconductor nanostructures also display morphology-dependent local surface plasmon resonance effect in the near-infrared region.[84] The morphology of the semiconductor substrate mainly affects its SERS performance through the following aspects:

(1) **Morphology design may induce specific structural resonance or enhanced light–matter interaction to boost the Raman signal.** Singh *et al.* synthesized MoS_2 nanoflowers by the hydrothermal method (Fig. 7a). They proposed that multi-reflection can take place under the incident light due to the existence of numerous nanosheets in the nanoflowers, which can enhance the electromagnetic radiation.[85] Ji *et al.* used hollow multi-shelled V_2O_5 microstructures as the SERS substrate, as shown in Fig. 7c and d. This platform exhibited excellent SERS performance because the unique structure possessed light-trapping effect and generated high electric field between inner and outer shells (Fig. 7e).[86]

(2) **Some unique structures, especially for sharp tip structure and tiny nanogaps, are conducive to the generation of Raman "hot spots", which can amplify the Raman signal effectively**. Fig. 7b shows the SEM image of a sea urchin-like MoO_3 nanostructure prepared by a chemical bath deposition method, which exhibits better SERS performance than the traditional 1D MoO_3 nanorod due to the existence of abundant sharp tips.[87] Ren *et al.* found that MoO_3/MoO_2 nanosheets with rough surface had excellent SERS performance due to the generation of strong electric field in the gap between adjacent MoO_3.[88] Therefore, we can carefully design the morphology of semiconductor substrates based on the above guidelines to improve their SERS performance.

In addition, rational morphology design can make SERS substrates provide more adsorption sites for target molecules, so the SERS performance can be further improved due to the concentration effect. For example, Singh *et al.* found that MoS_2 nanoflowers with large surface areas possess better SERS performance.[85]

3.2 Size adjustment

The size adjustment of semiconductors is also usually utilized to improve their SERS performance.[89,90] In this section, we analyze the effect of reducing the size of semiconductors to quantum dots and larger size semiconductor particles on SERS performance. The corresponding regulatory mechanism is summarized as follows:

(1) **The quantization of semiconductor nanoparticles mainly improves SERS performance by optimizing the charge transfer process**. When the size of the semiconductor nanoparticles is small enough to be quantum dots (especially when the nanoparticle size is smaller than the exciton Bohr radius), the exciton levels will split due to the quantum confinement effect.[67,89] The above phenomenon affects the energy level matching and charge transfer process between the semiconductor and probe molecules by changing the energy level structure of semiconductor nanoparticles, thereby regulating

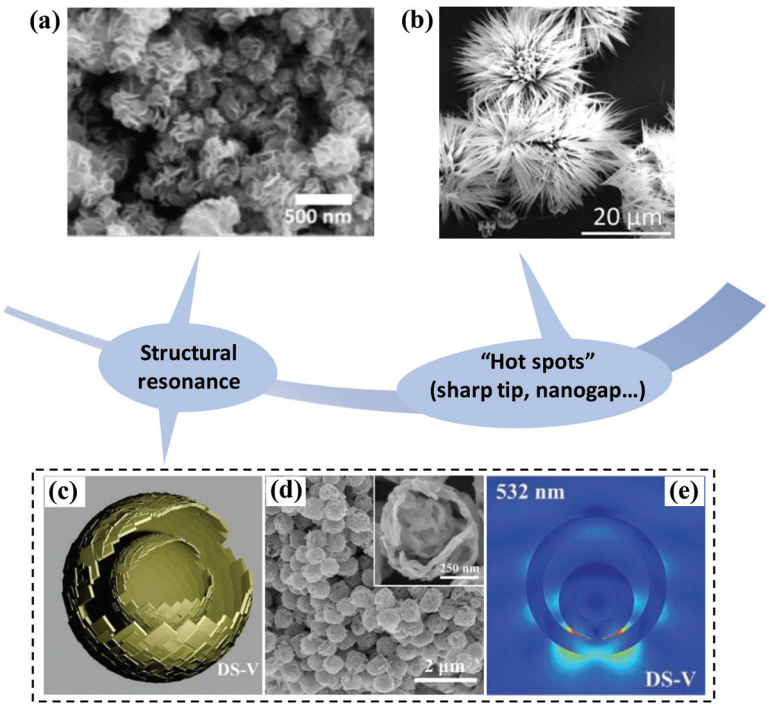

Fig. 7 (a) SEM image of MoS_2 nanoflowers. Reproduced with permission from ref. 85 (Copyright © 2020 Elsevier B.V. All rights reserved). (b) SEM image of a sea urchin-like MoO_3 nanostructure. Reproduced with permission from ref. 87 (Copyright © 2019, Royal Society of Chemistry). (c) Schematic demonstrating the microstructure of hollow multi-shelled V_2O_5. (d) SEM image of a hollow multi-shelled V_2O_5 microstructure; the inset is the enlarged SEM image. (e) Electromagnetic near-field distribution of single hollow multi-shelled V_2O_5 microstructure under 532 nm excitation. Reproduced with permission from ref. 86 (Copyright © 2021 Wiley-VCH GmbH).

the SERS performance of the semiconductor substrates.[91] Furthermore, compared with bulk materials, quantum dots possess larger surface area, allowing more probe molecules to adsorb on the surface. And the electrons on the quantum dots surface are weakly bound and can easily participate in the charge transfer process between the SERS substrate and probe molecules, thus improving SERS ability. Liu *et al.* prepared graphene quantum dots (P-GQDs) using a chemical vapor deposition method (Fig. 8a) and the size of P-GQDs can be well controlled by the growth temperature.[92] Compared with conventional graphene and highly oriented pyrolytic graphite, the P-GQDs exhibited stronger Raman enhancement ability, as shown in Fig. 8b. Interestingly, the SERS performance of P-GQDs showed size dependence, *i.e.* the P-GQDs with a diameter of 6.2 nm had the largest Raman enhancement due to the energy level matching between probe molecules and P-GQDs (Fig. 8c). Ta_2O_5 superstructure composed of numerous Ta_2O_5 quantum dots was synthesized *via* a simple hydrothermal method by Yang *et al.* Benefiting from the molecular resonance and charge transfer resonance, the Ta_2O_5 superstructure SERS substrate presented better Raman enhancement ability than bulk Ta_2O_5.[93]

(2) **Semiconductor nanoparticles with large size and high refractive index can generate Mie resonance under suitable excitation wavelength.**[94,95] Actually, one of the reasons for the low SERS sensitivity of most semiconductor materials is the lack of electromagnetic enhancement. For semiconductor materials, the Mie resonance effect can generate local electromagnetic field enhancement to improve the SERS performance. For example, Ji *et al.* synthesized submicrometer-sized spherical ZnO superstructures as a SERS substrate (Fig. 8d) and obtained Mie resonance on this substrate by tuning the superstructure size. They found that the enhancement factor of this ZnO superstructure SERS substrate exhibits obvious size dependence, as shown in Fig. 8e. The near-field electric field distribution of the ZnO superstructure with different diameters in Fig. 8f further shows the size dependence effect.[96] Therefore, we can realize electromagnetic enhancement on semiconductors by choosing suitable semiconductor materials and carefully tuning their size and structures.

3.3 Defect engineering

Defect engineering, as the most commonly used approach to improve the SERS performance of semiconductor materials, has been systematically studied. Currently, researchers mainly introduce defects in semiconductor materials through producing oxygen vacancies and element doping.[97–99]

(1) **On the one hand, defect engineering can promote the charge transfer process between the semiconductor substrates and probe molecules** because appropriate defects can change the energy level structure of the semiconductors by forming the surface defect state energy level. Making oxygen vacancies is an effective approach to obtain semiconductor substrates with great SERS performance. Researchers have successfully

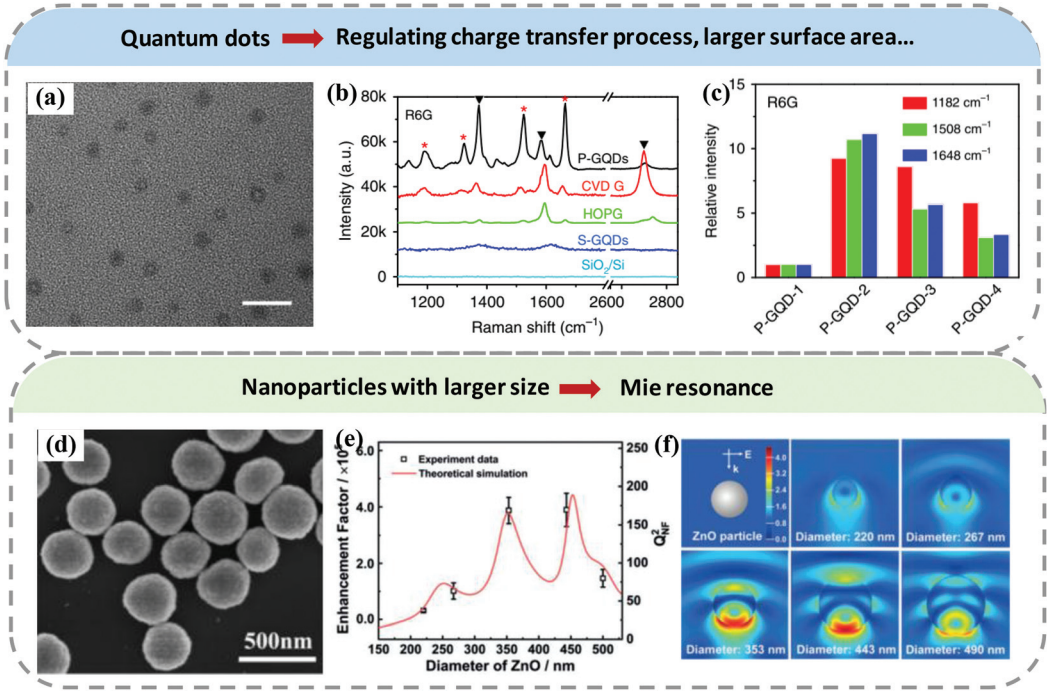

Fig. 8 (a) TEM image of graphene quantum dots. The scale bar is 20 nm. (b) SERS spectra of R6G molecules adsorbed on SiO_2/Si, GQDs prepared by solution method (S-GQDs), highly oriented pyrolytic graphite (HOPG), graphene (CVD G), and P-GQDs. (c) The comparison of Raman enhancement ability of P-GQDs with different diameters. Reproduced with permission from ref. 92 (Copyright © 2018, Springer Nature). (d) SEM image of ZnO superstructure. (e) The enhancement factor of different sizes of a ZnO superstructure. (f) Electric field distribution of ZnO superstructure with different diameters. Reproduced with permission from ref. 96 (Copyright © 2019 Wiley-VCH Verlag GmbH & Co. KGaA, Weinheim).

introduced oxygen vacancies in semiconductor materials *via* various methods, such as ion irradiation, lithium metal grinding reduction, and high temperature annealing under reducing gas atmosphere, *etc.*[100–102] Typically, Fan *et al.* employed WO_{3-x} rich in oxygen vacancies as a SERS substrate.[103] The oxygen vacancy played a critical role in improving the SERS performance of the WO_{3-x} substrate because it could form surface defect levels between the CB and VB of WO_{3-x}. The additional resonance caused by the oxygen vacancy resulted in the remarkable SERS performance (Fig. 9a and b). Conversely, Zheng *et al.* obtained SERS-active MoS_xO_y semiconductor substrate by oxygen incorporation.[104] The improved SERS performance was also attributed to the regulation of semiconductor energy levels by the oxygen incorporation process, which can promote the charge transfer process. Element doping (Co, Mg, Cu, H, *etc.*) is also adopted to improve the SERS performance. Zhou *et al.* synthesized Cu-doped SnO_2-NiO semiconductor SERS substrate and achieved very high enhancement factor (1.46×10^{10})[105] (Fig. 9c). They proved that Cu doping was beneficial to charge transfer resonance, Fig. 9d shows the energy level diagram of the probe molecules and SERS substrate.

(2) **On the other hand, defect engineering can introduce LSPR contribution in the semiconductor materials.** It has been reported that defects can modulate the carrier concentration of semiconductors, so proper defects can adjust the LSPR peak of the semiconductors in the far-infrared light region to the near-infrared or even visible light region, thereby introducing LSPR in the semiconductor materials. Zhao *et al.* first reported the surface plasmon resonance phenomenon in the doped semiconductors in 2009, which promoted the study of electromagnetic enhancement contribution in semiconductor materials to SERS.[106] Ye *et al.* obtained an oxygen vacancy-rich $W_{18}O_{49}$ mesocrystal by a rapid and green microwave synthetic method. They found that free electrons significantly increased because of the existence of a vast number of oxygen vacancies (Fig. 9e). Therefore, $W_{18}O_{49}$ exhibited a strong LSPR effect in the 400–800 nm range[25] (Fig. 9f). Apart from creating oxygen vacancies, by introducing gallium doping into ZnO nanoparticles, Wang *et al.* obtained Ga-doped ZnO nanoparticles with obvious surface plasmon resonance absorption in the visible-NIR region.[107] They found that electromagnetic enhancement played a key role in the Raman enhancement for this SERS substrate. And proper doping concentration was conducive to the increase of carrier concentration, resulting in stronger surface plasmon resonance absorption and SERS enhancement (Fig. 9g and h). Therefore, utilizing rational defect engineering, we can improve the SERS performance of semiconductor substrates by promoting the charge transfer process and introducing the LSPR effect.

3.4 Crystallinity

Different crystallinity of semiconductors will also affect the SERS performance by regulating the charge transfer process.[23,108] Usually, the crystalline semiconductors have

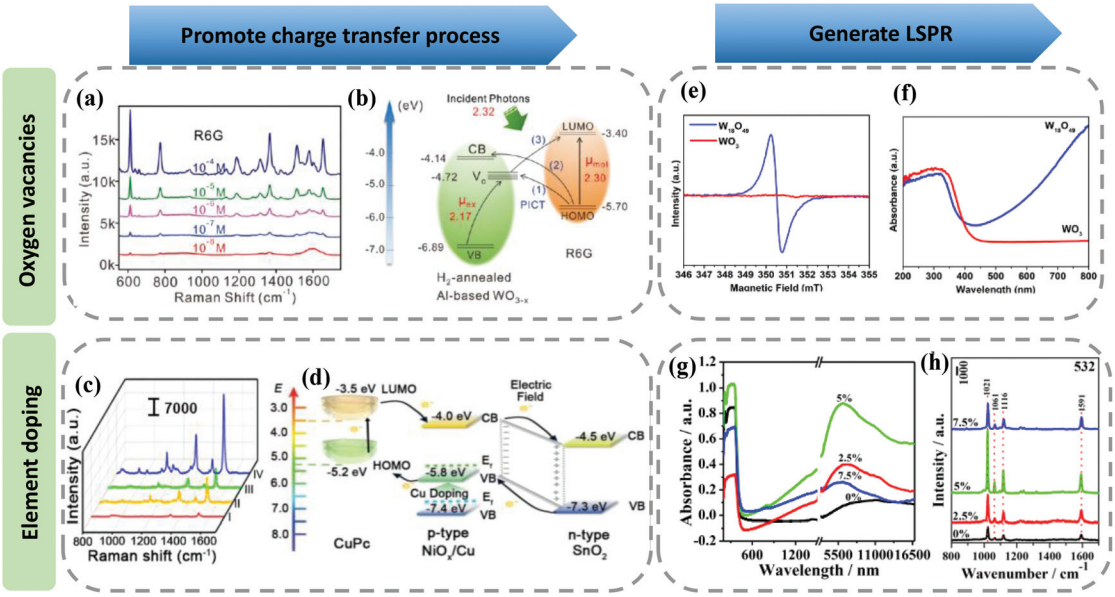

Fig. 9 (a) SERS spectra of R6G molecules adsorbed on WO_{3-x} substrate at different concentrations. (b) Schematic showing the energy level diagram of R6G on WO_{3-x} and the charge transfer process in this system. Reproduced with permission from ref. 103 (Copyright © 2019 WILEY-VCH Verlag GmbH & Co. KGaA, Weinheim). (c) SERS spectra of copper phthalo-cyanine (CuPc) molecules on Si(I), SnO_2 (II), SnO_2-NiO (III), and Cu-doped SnO_2-NiO (IV) substrates. (d) Schematic presenting the energy level diagram of CuPc on Cu-doped SnO_2-NiO and the charge transfer process. Reproduced with permission from ref. 105 (Copyright © 2021 Wiley-VCH GmbH). (e) Electron paramagnetic resonance (EPR) spectra of the $W_{18}O_{49}$ and WO_3 mesocrystals. (f) UV-vis spectra of $W_{18}O_{49}$ and WO_3 mesocrystals. Reproduced with permission from ref. 25 (Copyright © 2021, American Chemical Society). (g) FTIR absorption spectra of Ga-doped ZnO nanoparticles combined with the UV-vis-NIR absorption spectra. (h) SERS spectra of MPy on Ga-doped ZnO substrate with different doping ratios. Reproduced with permission from ref. 107 (Copyright © 2021, American Chemical Society).

ordered and periodic lattice structures, which may restrict the electron transfer. In contrast, the long-range disordered structure of amorphous semiconductors facilitates the electron transfer process. Wang *et al.* systematically studied this effect. In 2017, they first observed ultrahigh SERS activity in amorphous ZnO nanocages (a-ZnO NCs).[109] They explored the possible enhancement mechanism of a-ZnO NCs using density functional theory simulations. Compared with crystalline ZnO nanocages (c-ZnO NCs), the electronic state of a-ZnO NCs was a metastable state, so the surface electrons were easily transferred, resulting in a more effective charge transfer process. Based on this finding, they further developed amorphous Rh_3S_6 as a highly sensitive SERS substrate (Fig. 10a).[110] They proposed that the excellent sensitivity could be ascribed to the quasi-resonance Raman effect and multiple light scattering, as shown in Fig. 10b. In 2019, they studied the SERS performance of amorphous TiO_2 nanosheets (a-TiO_2 NSs) and crystalline TiO_2 nanosheets (c-TiO_2 NSs), and the former exhibited stronger SERS activity. Fig. 10c clearly shows the SERS spectra comparison of a-TiO_2 NSs and c-TiO_2 NSs for 4-MBA molecules. On the one hand, they found that a-TiO_2 NSs possessed relatively narrow band gap and higher electronic density of states, which facilitated stronger vibronic coupling. And the improved vibronic coupling could promote the charge transfer resonance, as shown in Fig. 10d. In addition, the a-TiO_2 NSs had higher electrostatic potential because of the existence of abundant low coordination Ti atoms and oxygen defects, and this can also induce larger charge transfer.[29] Another amorphous semiconductor nanomaterials, such as H_xMoO_3 quantum dots and $M(OH)_x$ (M = Fe, Co, Ni) also displayed excellent SERS performance.[111–113]

3.5 Phase structure

Some semiconductor materials have multiple phase structures, so studying the phase structure dependence of SERS performance is helpful in optimizing the SERS activity.[114,115] Typically, the MoX_2 (X = S, Se, *etc.*) involves semiconducting 2H-phase and metallic 1T-phase, and they present different electrochemical properties. Yin *et al.* demonstrated that the SERS performance of 1T-MoX_2 (X = S, Se) is superior to 2H-MoX_2, as shown in Fig. 11a. According to experimental results and theoretical analysis, they speculated the possible reason for the better SERS performance of 1T-MoX_2 (taking $MoSe_2$ as example) (Fig. 11b), *i.e.* no extra energy was required when the electrons jumped from Fermi energy level of the 1T-$MoSe_2$ to the HOMO level of molecules, resulting in more efficient charge transfer process than 2H-$MoSe_2$ (electrons required 0.065 eV energy when transferred from top of the valence band (TVB) of 2H-$MoSe_2$ to HOMO level of molecules).[116] TiO_2 is also a typical multiple phase material (anatase, rutile, and brookite phase). Yang *et al.* compared the SERS performance of TiO_2 nanoparticles with different phase structure. They found that TiO_2 nanoparticles with mixed phase structure (anatase phase: 85%, rutile phase: 15%) exhibited optimal

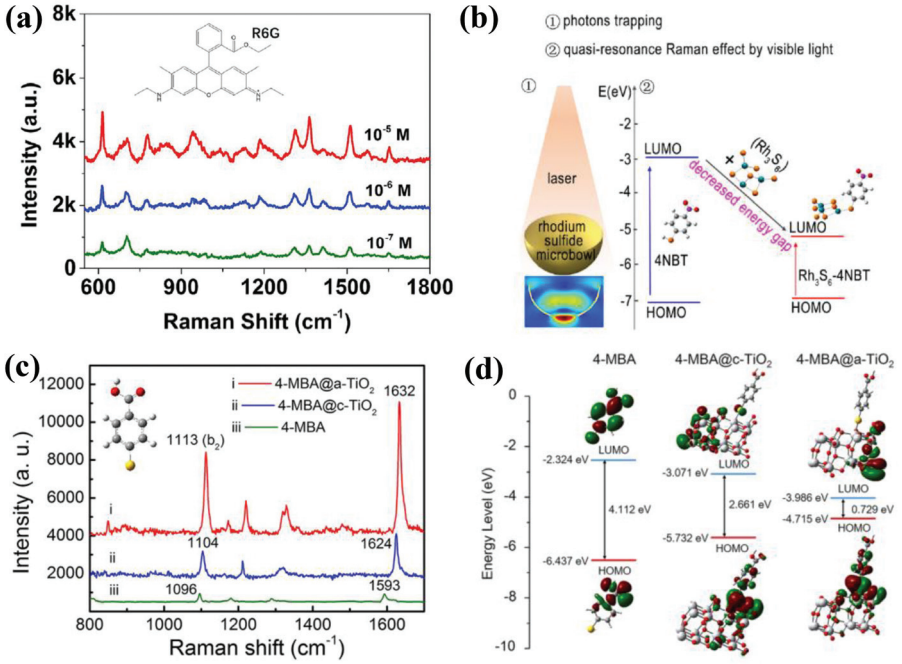

Fig. 10 (a) SERS spectra of R6G molecules adsorbed on amorphous Rh_3S_6 substrate at different concentrations. (b) Enhancement mechanism of the Rh_3S_6 microbowl substrate. Reproduced with permission from ref. 110 (Copyright © 2018 The Author(s)). (c) SERS spectra of 4-MBA on amorphous and crystalline TiO_2 nanosheets. (d) The energy level diagram of 4-MBA, 4-MBA@ crystalline TiO_2, and 4-MBA@ amorphous TiO_2. Reproduced with permission from ref. 29 (Copyright © 2019, American Chemical Society).

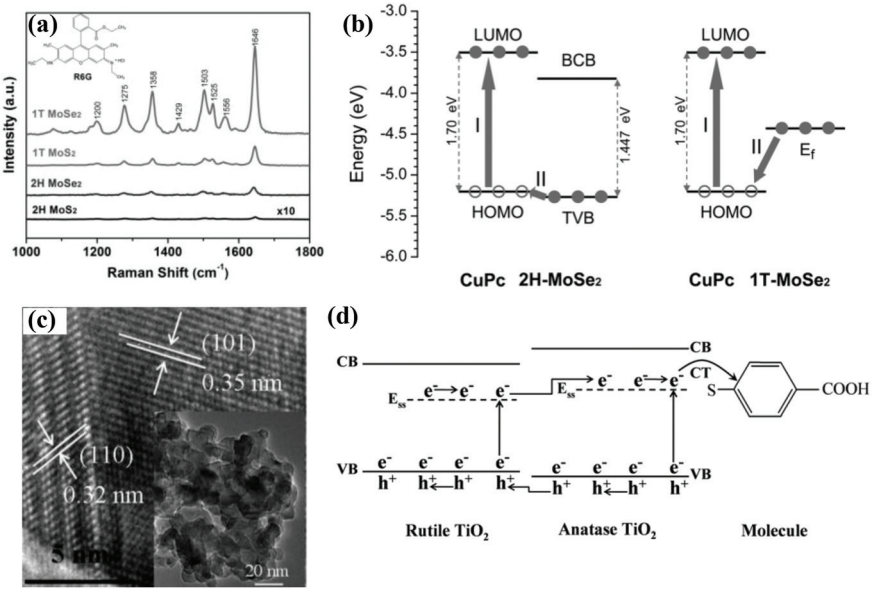

Fig. 11 (a) SERS spectra of R6G on 1T $MoSe_2$, 1T MoS_2, 2H $MoSe_2$, and 2H MoS_2 substrates. (b) The energy level diagram and charge transfer process of CuPc molecules on 2H and 1T $MoSe_2$. Reproduced with permission from ref. 116 (Copyright © 2017 WILEY-VCH Verlag GmbH & Co. KGaA, Weinheim). (c) High-resolution TEM image of TiO_2 nanoparticles; the inset is a low magnification TEM image. (d) The charge transfer process of probe molecules adsorbed on the mixed phase TiO_2 nanoparticles. Reproduced with permission from ref. 117 (Copyright © 2015 John Wiley & Sons, Ltd).

SERS performance. Fig. 11c displays the TEM image of the mixed phase TiO_2. In this mixed phase structure TiO_2, the holes tend to transfer from anatase to rutile phase while the electrons follow a reverse transfer path (Fig. 11d). Therefore, apart from the charge transfer enhancement of intrinsic anatase TiO_2, the synergy between the two phases provides

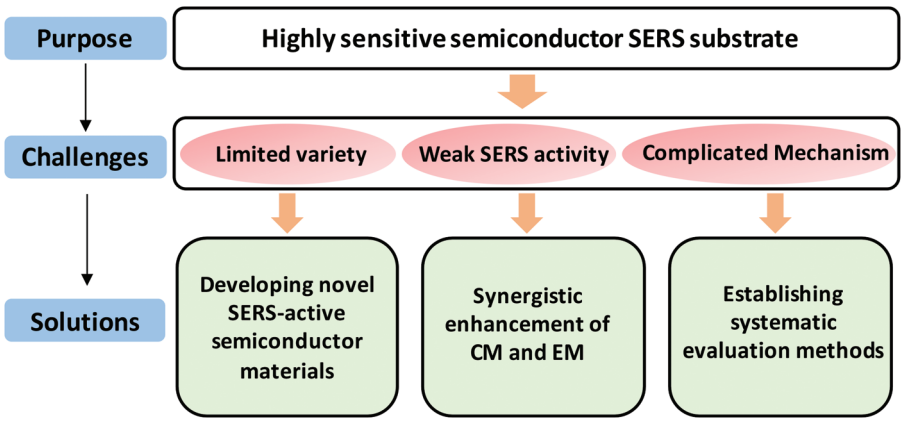

Fig. 12 The challenges and possible solutions in the field of semiconductor SERS.

additional charge transfer.[117] Therefore, in addition to focusing on the impact of some main factors (morphology, size, defect, and crystallinity) on the SERS performance, we can also optimize its SERS performance by selecting appropriate semiconductor phase structure.

4 Conclusions and outlook

As a powerful spectroscopic technique with the advantages of high sensitivity, fingerprint specificity, and fast and non-destructive detection, SERS has shown great application potential in various fields. The construction of high-performance SERS substrates is key to promoting their practical applications. For a long time, SERS substrates based on noble metal materials have been dominant. However, in view of the bottleneck of noble metal SERS substrates, semiconductor SERS substrates have been developed and extensively studied. In this review, we summarized several main types of semiconductor SERS substrates, as well as the strategies to further improve the SERS performance of semiconductor substrates.

Although semiconductor SERS substrates possess obvious merits compared to noble metal SERS substrates, and a large number of SERS-active semiconductor nanomaterials have been successfully fabricated with the efforts of researchers, there are still some challenges as follows: (1) The most fatal shortcoming of semiconductor SERS substrates is the weak Raman enhancement because chemical enhancement plays a major role in semiconductors. At present, the SERS sensitivity of most semiconductor substrates is low, which is difficult to meet the needs of practical applications. (2) Most studies improved SERS performance of semiconductor substrates by enhancing the charge transfer resonance, and the improvement ability is limited. Research on boosting the SERS ability of semiconductors by regulating the electromagnetic enhancement is relatively lacking. (3) Currently, the types of SERS-active semiconductor materials are limited because the research started relatively late. More potential semiconductor materials are worth developing. (4) The Raman enhancement mechanism of semiconductor SERS substrates is complicated and the research on it remains to be deepened and improved.

Therefore, developing novel SERS-active semiconductor materials, introducing electromagnetic enhancement, or even utilizing the synergistic effects of the CM and EM to boost the Raman enhancement ability, and elucidating the SERS mechanism by effective means are meaningful to promote the development and practical applications of high-performance semiconductor SERS substrates. Fig. 12 shows the challenges and possible solutions in the field of semiconductor SERS.

Author contributions

Xuejiao Wang: Conceptualization, formal analysis, data curation, investigation, writing – original draft. Erjin Zhang: Writing – review and editing, funding acquisition, project administration. Huimin Shi: Formal analysis, data curation. Yufeng Tao: Formal analysis, data curation. Xudong Ren: Writing – review and editing, supervision, funding acquisition.

Conflicts of interest

There are no conflicts to declare.

Acknowledgements

We gratefully acknowledge the financial support from the Natural Science Foundation of Jiangsu (BK20210746, BK20210781) and the National Natural Science Foundation of China (No. 52102259).

References

1 M. Fleischmann, P. J. Hendra and A. J. Mcquillan, *Chem. Phys. Lett.*, 1974, **26**, 163–166.

2 J. Perumal, Y. Wang, A. B. E. Attia, U. Dinish and M. Olivo, *Nanoscale*, 2021, **13**, 553–580.
3 Y. X. Leong, Y. H. Lee, C. S. L. Koh, G. C. Phan-Quang, X. Han, I. Y. Phang and X. Y. Ling, *Nano Lett.*, 2021, **21**, 2642–2649.
4 Y. C. Kao, X. Han, Y. H. Lee, H. K. Lee, G. C. Phan-Quang, C. L. Lay, H. Y. F. Sim, V. J. X. Phua, L. S. Ng, C. W. Ku, T. C. Tan, I. Y. Phang, N. S. Tan and X. Y. Ling, *ACS Nano*, 2020, **14**, 2542–2552.
5 H. Feng, Q. Fu, W. Du, R. Zhu, X. Ge, C. Wang, Q. Li, L. Su, H. Yang and J. Song, *ACS Nano*, 2021, **15**, 3402–3414.
6 J. Shan, Y. Zhang, J. Wang, T. Ren, M. Jin and X. Wang, *J. Hazard. Mater.*, 2020, **400**, 123202.
7 C. S. L. Koh, H. K. Lee, X. Han, H. Y. F. Sim and X. Y. Ling, *Chem. Commun.*, 2018, **54**, 2546–2549.
8 L. Wu, H. Pu, L. Huang and D.-W. Sun, *Food Chem.*, 2020, **328**, 127105.
9 Y. Chen, H. Liu, Y. Tian, Y. Du, Y. Ma, S. Zeng, C. Gu, T. Jiang and J. Zhou, *ACS Appl. Mater. Interfaces*, 2020, **12**, 14386–14399.
10 A. Alyami, A. Mirabile and D. Iacopino, *Heritage Sci.*, 2019, **7**, 1–10.
11 X. X. Han, W. Ji, B. Zhao and Y. Ozaki, *Nanoscale*, 2017, **9**, 4847–4861.
12 V. Rajput, R. K. Gupta and J. Prakash, *J. Mater. Chem. C*, 2022, **10**, 73–95.
13 G. Demirel, H. Usta, M. Yilmaz, M. Celik, H. A. Alidagi and F. Buyukserin, *J. Mater. Chem. C*, 2018, **6**, 5314–5335.
14 W. Ji, B. Zhao and Y. Ozaki, *J. Raman Spectrosc.*, 2016, **47**, 51–58.
15 R. Haldavnekar, K. Venkatakrishnan and B. Tan, *Nat. Commun.*, 2018, **9**, 1–18.
16 B. Yang, S. Jin, S. Guo, Y. Park, L. Chen, B. Zhao and Y. M. Jung, *ACS Omega*, 2019, **4**, 20101–20108.
17 L. Tao, K. Chen, Z. Chen, C. Cong, C. Qiu, J. Chen, X. Wang, H. Chen, T. Yu and W. Xie, *J. Am. Chem. Soc.*, 2018, **140**, 8696–8704.
18 J. Yao, Y. Quan, R. Gao, J. Li, L. Chen, Y. Liu, J. Lang, H. Shen, Y. Wang and J. Yang, *Langmuir*, 2019, **35**, 8921–8926.
19 Y. Quan, J. Yao, S. Yang, L. Chen, Y. Liu, J. Lang, H. Zeng, J. Yang and M. Gao, *J. Hazard. Mater.*, 2020, **391**, 122222.
20 X. Wang, G. She, H. Xu, L. Mu and W. Shi, *Sens. Actuators, B*, 2014, **193**, 745–751.
21 J. R. Lombardi and R. L. Birke, *J. Phys. Chem. C*, 2014, **118**, 11120–11130.
22 H. K. Lee, Y. H. Lee, C. S. L. Koh, G. C. Phan-Quang, X. Han, C. L. Lay, H. Y. F. Sim, Y. C. Kao, Q. An and X. Y. Ling, *Chem. Soc. Rev.*, 2019, **48**, 731–756.
23 X. Wang and L. Guo, *Angew. Chem., Int. Ed.*, 2020, **59**, 4231–4239.
24 J. M. Luther, P. K. Jain, T. Ewers and A. P. Alivisatos, *Nat. Mater.*, 2011, **10**, 361–366.
25 Y. Ye, C. Chen, W. Li, X. Guo, H. Yang, H. Guan, H. Bai, W. Liu and G. Xi, *Anal. Chem.*, 2021, **93**, 3138–3145.
26 D. Maznichenko, K. Venkatakrishnan and B. Tan, *J. Phys. Chem. C*, 2012, **117**, 578–583.
27 A. I. Kuznetsov, A. E. Miroshnichenko, M. L. Brongersma, Y. S. Kivshar and B. Luk'yanchuk, *Science*, 2016, **354**, DOI: 10.1126/science.aag2472.
28 S. Hayashi, R. Koh, Y. Ichiyama and K. Yamamoto, *Phys. Rev. Lett.*, 1988, **60**, 1085–1088.
29 X. Wang, W. Shi, S. Wang, H. Zhao, J. Lin, Z. Yang, M. Chen and L. Guo, *J. Am. Chem. Soc.*, 2019, **141**, 5856–5862.
30 B. Yang, Y. Wang, S. Guo, S. Jin, E. Park, L. Chen and Y. M. Jung, *Bull. Korean Chem. Soc.*, 2021, **42**, 1411–1418.
31 A. Musumeci, D. Gosztola, T. Schiller, N. M. Dimitrijevic, V. Mujica, D. Martin and T. Rajh, *J. Am. Chem. Soc.*, 2009, **131**, 6040–6041.
32 Y. Liu, H. Ma, X. X. Han and B. Zhao, *Mater. Horiz.*, 2021, **8**, 370–382.
33 H. Wu, H. Wang and G. Li, *Analyst*, 2017, **142**, 326–335.
34 T. Takagahara and K. Takeda, *Phys. Rev. B: Condens. Matter Mater. Phys.*, 1992, **46**, 15578–15581.
35 L. E. Brus, *J. Chem. Phys.*, 1984, **80**, 4403–4409.
36 S. E. Bell, G. Charron, E. Cortés, J. Kneipp, M. L. de la Chapelle, J. Langer, M. Procházka, V. Tran and S. Schlücker, *Angew. Chem., Int. Ed.*, 2020, **59**, 5454–5462.
37 H. Yamada, Y. Yamamoto and N. Tani, *Chem. Phys. Lett.*, 1982, **86**, 397–400.
38 H. Yamada and Y. Yamamoto, *Surf. Sci.*, 1983, **134**, 71–90.
39 C. Liu, Q. Song, J. Chen, X. Li, J. Cai, Z. Lu, W. Li, N. X. Fang and S. P. Feng, *Adv. Mater. Interfaces*, 2019, **6**, 1900534.
40 E. Proniewicz, A. Tata, A. Wojcik, M. Starowicz, J. Pacek and M. Molenda, *Phys. Chem. Chem. Phys.*, 2020, **22**, 28100–28114.
41 J. Lin, J. Yu, O. U. Akakuru, X. Wang, B. Yuan, T. Chen, L. Guo and A. Wu, *Chem. Sci.*, 2020, **11**, 9414–9420.
42 B. P. Majee and A. K. Mishra, *Mater. Res. Express*, 2020, **6**, 1250j1.
43 H. A. O. Wen, *Mol. Phys.*, 1996, **88**, 281–290.
44 Q. Liu, L. Jiang and L. Guo, *Small*, 2014, **10**, 48–51.
45 H. Zhang, S. Huang, X. Yang, R. Yuan and Y. Chai, *Sens. Actuators, B*, 2021, **343**, 130142.
46 L. Yang, Y. Peng, Y. Yang, J. Liu, Z. Li, Y. Ma, Z. Zhang, Y. Wei, S. Li, Z. Huang and N. V. Long, *ACS Appl. Nano Mater.*, 2018, **1**, 4516–4527.
47 X. Li, Y. Shang, J. Lin, A. Li, X. Wang, B. Li and L. Guo, *Adv. Funct. Mater.*, 2018, **28**, 1801868.
48 J. Li, H. Bai, J. Zhai, W. Li, W. Fan and G. Xi, *Chem. Commun.*, 2019, **55**, 4679–4682.
49 L. Yang, Y. Peng, Y. Yang, J. Liu, H. Huang, B. Yu, J. Zhao, Y. Lu, Z. Huang, Z. Li and J. R. Lombardi, *Adv. Sci.*, 2019, **6**, 1900310.
50 L. Yang, Y. Wei, Y. Song, Y. Peng, Y. Yang and Z. Huang, *Mater. Des.*, 2020, **193**, 108808.
51 X. Ling, L. Xie, Y. Fang, H. Xu, H. Zhang, J. Kong, M. S. Dresselhaus, J. Zhang and Z. Liu, *Nano Lett.*, 2009, **10**, 553–561.

52 J. Seo, J. Lee, Y. Kim, D. Koo, G. Lee and H. Park, *Nano Lett.*, 2020, **20**, 1620–1630.
53 X. Pan, L. Li, H. Lin, J. Tan, H. Wang, M. Liao, C. Chen, B. Shan, Y. Chen and M. Li, *Biosens. Bioelectron.*, 2019, **145**, 111713.
54 S. A. Ghopry, M. A. Alamri, R. Goul, R. Sakidja and J. Z. Wu, *Adv. Opt. Mater.*, 2019, **7**, 1801249.
55 H. Cui, S. Li, S. Deng, H. Chen and C. Wang, *ACS Sens.*, 2017, **2**, 386–393.
56 E. Er, H.-L. Hou, A. Criado, J. Langer, M. Möller, N. Erk, L. M. Liz-Marzán and M. Prato, *Chem. Mater.*, 2019, **31**, 5725–5734.
57 D. Yan, W. Qiu, X. Chen, L. Liu, Y. Lai, Z. Meng, J. Song, Y. Liu, X.-Y. Liu and D. Zhan, *J. Phys. Chem. C*, 2018, **122**, 14467–14473.
58 M. Li, Y. Gao, X. Fan, Y. Wei, Q. Hao and T. Qiu, *Nanoscale Horiz.*, 2021, **6**, 186–191.
59 C. Weng, Y. Luo, B. Wang, J. Shi, L. Gao, Z. Cao and G. Duan, *J. Mater. Chem. C*, 2020, **8**, 14138–14145.
60 X. Song, Y. Wang, F. Zhao, Q. Li, H. Q. Ta, M. H. Rummeli, C. G. Tully, Z. Li, W. J. Yin, L. Yang, K. B. Lee, J. Yang, I. Bozkurt, S. Liu, W. Zhang and M. Chhowalla, *ACS Nano*, 2019, **13**, 8312–8319.
61 X. Li, S. Guo, J. Su, X. Ren and Z. Fang, *ACS Appl. Mater. Interfaces*, 2020, **12**, 28474–28483.
62 L. Tao, K. Chen, Z. Chen, C. Cong, C. Qiu, J. Chen, X. Wang, H. Chen, T. Yu, W. Xie, S. Deng and J. B. Xu, *J. Am. Chem. Soc.*, 2018, **140**, 8696–8704.
63 P. Karthick Kannan, P. Shankar, C. Blackman and C. H. Chung, *Adv. Mater.*, 2019, **31**, 1803432.
64 P. Miao, J. K. Qin, Y. Shen, H. Su, J. Dai, B. Song, Y. Du, M. Sun, W. Zhang, H. L. Wang, C. Y. Xu and P. Xu, *Small*, 2018, **14**, e1704079.
65 G. Demirel, R. L. Gieseking, R. Ozdemir, S. Kahmann, M. A. Loi, G. C. Schatz, A. Facchetti and H. Usta, *Nat. Commun.*, 2019, **10**, 1–9.
66 S. Ganesh, K. Venkatakrishnan and B. Tan, *Nat. Commun.*, 2020, **11**, 1–15.
67 X. Xue, W. Ji, Z. Mao, H. Mao, Y. Wang, X. Wang, W. Ruan, B. Zhao and J. R. Lombardi, *J. Phys. Chem. C*, 2012, **116**, 8792–8797.
68 Y. Wang, W. Ruan, J. Zhang, B. Yang, W. Xu, B. Zhao and J. R. Lombardi, *J. Raman Spectrosc.*, 2009, **40**, 1072–1077.
69 Y. Wang, H. Hu, S. Jing, Y. Wang, Z. Sun, B. Zhao, C. Zhao and J. R. Lombardi, *Anal. Sci.*, 2007, **23**, 787–791.
70 Y. Wang, Z. Sun, Y. Wang, H. Hu, B. Zhao, W. Xu and J. R. Lombardi, *Spectrochim. Acta, Part A*, 2007, **66**, 1199–1203.
71 T. Wang, S. Wang, Z. Cheng, J. Wei, L. Yang, Z. Zhong, H. Hu, Y. Wang, B. Zhou and P. Li, *Chem. Eng. J.*, 2021, **424**, 130323.
72 L. Wang, S. Patskovsky, B. Gauthier-Soumis and M. Meunier, *Small*, 2022, 2105209.
73 Z. Lao, Y. Zheng, Y. Dai, Y. Hu, J. Ni, S. Ji, Z. Cai, Z. J. Smith, J. Li and L. Zhang, *Adv. Funct. Mater.*, 2020, **30**, 1909467.
74 Q. Zhao, H. Yang, B. Nie, Y. Luo, J. Shao and G. Li, *ACS Appl. Mater. Interfaces*, 2022, **14**, 3580–3590.
75 C. Qiu, Y. Bao, N. L. Netzer and C. Jiang, *J. Mater. Chem. A*, 2013, **1**, 8790–8797.
76 H. L. Wu, X. B. Li, C. H. Tung and L. Z. Wu, *Adv. Mater.*, 2019, **31**, e1900709.
77 M. Shafi, M. Zhou, P. Duan, W. Liu, W. Zhang, Z. Zha, J. Gao, S. Wali, S. Jiang and B. Man, *Sens. Actuators, B*, 2022, 131360.
78 C. Muehlethaler, A. Odate, J. L. Weyher, I. Dzięcielewski and J. R. Lombardi, *Appl. Surf. Sci.*, 2018, **457**, 809–814.
79 S. Zhao, H. Wang, L. Niu, W. Xiong, Y. Chen, M. Zeng, S. Yuan and L. Fu, *Small*, 2021, **17**, 2103442.
80 G. Song, W. Gong, S. Cong and Z. Zhao, *Angew. Chem., Int. Ed.*, 2021, **60**, 5505–5511.
81 Y. Ye, C. Chen, H. Bai, W. Liu, W. Li, J. Li, W. Yi and G. Xi, *Cell Rep. Phys. Sci.*, 2020, **1**, 100031.
82 Z. Tian, H. Bai, C. Chen, Y. Ye, Q. Kong, Y. Li, W. Fan, W. Yi and G. Xi, *iScience*, 2019, **19**, 836–849.
83 X. Fu, F. Bei, X. Wang, X. Yang and L. Lu, *J. Raman Spectrosc.*, 2009, **40**, 1290–1295.
84 W. Li, R. Zamani, P. Rivera Gil, B. Pelaz, M. Ibanez, D. Cadavid, A. Shavel, R. A. Alvarez-Puebla, W. J. Parak, J. Arbiol and A. Cabot, *J. Am. Chem. Soc.*, 2013, **135**, 7098–7101.
85 J. Singh, Rishikesh, S. Kumar and R. K. Soni, *J. Alloys Compd.*, 2020, **849**, 156502.
86 W. Ji, L. Li, J. Guan, M. Mu, W. Song, L. Sun, B. Zhao and Y. Ozaki, *Adv. Opt. Mater.*, 2021, **9**, 2101866.
87 R. Prabhu B., K. Bramhaiah, K. K. Singh and N. S. John, *Nanoscale Adv.*, 2019, **1**, 2426–2434.
88 P. Ren, W. Zhou, X. Ren, X. Zhang, B. Sun, Y. Chen, Q. Zheng, J. Li and W. Zhang, *Nanotechnology*, 2020, **31**, 224002.
89 X. Fu, Y. Pan, X. Wang and J. R. Lombardi, *J. Chem. Phys.*, 2011, **134**, 024707.
90 J. Pan, M. Li, Y. Y. Luo, H. Wu, L. Zhong, Q. Wang and G. H. Li, *Appl. Surf. Sci.*, 2015, **333**, 34–38.
91 S. K. Islam, M. A. Sohel and J. R. Lombardi, *J. Phys. Chem. C*, 2014, **118**, 19415–19421.
92 D. Liu, X. Chen, Y. Hu, T. Sun, Z. Song, Y. Zheng, Y. Cao, Z. Cai, M. Cao, L. Peng, Y. Huang, L. Du, W. Yang, G. Chen, D. Wei, A. T. S. Wee and D. Wei, *Nat. Commun.*, 2018, **9**, 193.
93 L. Yang, Y. Yang, J. R. Lombardi, Y. Peng and Z. Huang, *Appl. Surf. Sci.*, 2020, **520**, 146325.
94 P. A. Dmitriev, D. G. Baranov, V. A. Milichko, S. V. Makarov, I. S. Mukhin, A. K. Samusev, A. E. Krasnok, P. A. Belov and Y. S. Kivshar, *Nanoscale*, 2016, **8**, 9721–9726.
95 D. Christie, J. Lombardi and I. Kretzschmar, *J. Phys. Chem. C*, 2014, **118**, 9114–9118.
96 W. Ji, L. Li, W. Song, X. Wang, B. Zhao and Y. Ozaki, *Angew. Chem., Int. Ed.*, 2019, **58**, 14452–14456.
97 H. Guan, Z. Tian, Q. Kong and G. Xi, *Chem. Commun.*, 2021, **57**, 4815–4818.

98 C. Gu, D. Li, S. Zeng, T. Jiang, X. Shen and H. Zhang, *Nanoscale*, 2021, **13**, 5620–5651.
99 Y. Peng, C. Lin, M. Tang, L. Yang, Y. Yang, J. Liu, Z. Huang and Z. Li, *Appl. Surf. Sci.*, 2020, **509**, 145376.
100 X.-D. Zheng, F. Ren, H.-Y. Wu, W.-J. Qin and C.-Z. Jiang, *Nanotechnology*, 2018, **29**, 155301.
101 Y. Cao, P. Liang, Q. Dong, D. Wang, D. Zhang, L. Tang, L. Wang, S. Jin, D. Ni and Z. Yu, *Anal. Chem.*, 2019, **91**, 8683–8690.
102 D. Luo, Z. Zhang, G. Li, S. Cheng, S. Li, J. Li, R. Gao, M. Li, S. Sy and Y.-P. Deng, *ACS Nano*, 2020, **14**, 4849–4860.
103 X. Fan, M. Li, Q. Hao, M. Zhu, X. Hou, H. Huang, L. Ma, O. G. Schmidt and T. Qiu, *Adv. Mater. Interfaces*, 2019, **6**, 1901133.
104 Z. Zheng, S. Cong, W. Gong, J. Xuan, G. Li, W. Lu, F. Geng and Z. Zhao, *Nat. Commun.*, 2017, **8**, 1993.
105 Y. Zhou, Q. Gu, T. Qiu, X. He, J. Chen, R. Qi, R. Huang, T. Zheng and Y. Tian, *Angew. Chem.*, 2021, **133**, 26464–26471.
106 Y. Zhao, H. Pan, Y. Lou, X. Qiu, J. Zhu and C. Burda, *J. Am. Chem. Soc.*, 2009, **131**, 4253–4261.
107 Y. Wang, M. Zhang, H. Ma, H. Su, A. Li, W. Ruan and B. Zhao, *ACS Appl. Mater. Interfaces*, 2021, **13**, 35038–35045.
108 J. Lin, W. Ren, A. Li, C. Yao, T. Chen, X. Ma, X. Wang and A. Wu, *ACS Appl. Mater. Interfaces*, 2020, **12**, 4204–4211.
109 X. Wang, W. Shi, Z. Jin, W. Huang, J. Lin, G. Ma, S. Li and L. Guo, *Angew. Chem., Int. Ed.*, 2017, **56**, 9851–9855.
110 A. Li, J. Lin, Z. Huang, X. Wang and L. Guo, *iScience*, 2018, **10**, 1–10.
111 M. Gao, P. Miao, X. Han, C. Sun, Y. Ma, Y. Gao and P. Xu, *Inorg. Chem. Front.*, 2019, **6**, 2318–2324.
112 H. Li, Q. Xu, X. Wang and W. Liu, *Small*, 2018, **14**, e1801523.
113 A. Li, J. Yu, J. Lin, M. Chen, X. Wang and L. Guo, *J. Phys. Chem. Lett.*, 2020, **11**, 1859–1866.
114 R. Su, Y. Quan, S. Yang, M. Hu, J. Yang and M. Gao, *J. Alloys Compd.*, 2021, **886**, 161268.
115 P. Miao, J. Wu, Y. Du, Y. Sun and P. Xu, *J. Mater. Chem. C*, 2018, **6**, 10855–10860.
116 Y. Yin, P. Miao, Y. Zhang, J. Han, X. Zhang, Y. Gong, L. Gu, C. Xu, T. Yao, P. Xu, Y. Wang, B. Song and S. Jin, *Adv. Funct. Mater.*, 2017, **27**, 1606694.
117 L. Yang, M. Gong, X. Jiang, D. Yin, X. Qin, B. Zhao and W. Ruan, *J. Raman Spectrosc.*, 2015, **46**, 287–292.